

44. **Thomas ME, Brunskill NJ, Harris KP, Bailey E, Pringle JH, Furness PN, and Walls J.** Proteinuria induces tubular cell turnover: A potential mechanism for tubular atrophy. *Kidney Int* 55: 890-898, 1999.
45. **Valencia JV, Mone M, Koehne C, Rediske J, and Hughes TE.** Binding of receptor for advanced glycation end products (RAGE) ligands is not sufficient to induce inflammatory signals: lack of activity of endotoxin-free albumin-derived advanced glycation end products. *Diabetologia* 47: 844-852, 2004.
46. **Wang Y, Rangan GK, Tay YC, Wang Y, and Harris DC.** Induction of monocyte chemoattractant protein-1 by albumin is mediated by nuclear factor kappaB in proximal tubule cells. *J Am Soc Nephrol* 10: 1204-1213, 1999.
47. **Winterbourn CC.** Comparative reactivities of various biological compounds with myeloperoxidase-hydrogen peroxide-chloride, and similarity of the oxidant to hypochlorite. *Biochim Biophys Acta* 840: 204-210, 1985.
48. **Witko-Sarsat V, Friedlander M, Capeillere-Blandin C, Nguyen-Khoa T, Nguyen AT, Zingraff J, Jungers P, and Descamps-Latscha B.** Advanced oxidation protein products as a novel marker of oxidative stress in uremia. *Kidney Int* 49: 1304-1313, 1996.
49. **Witko-Sarsat V, Friedlander M, Nguyen Khoa T, Capeillere-Blandin C, Nguyen AT, Canteloup S, Dayer JM, Jungers P, Drueke T, and Descamps-Latscha B.** Advanced oxidation protein products as novel mediators of inflammation and monocyte activation in chronic renal failure. *J Immunol* 161: 2524-2532, 1998.
50. **Yang YL, Lin SH, Chuang LY, Guh JY, Liao TN, Lee TC, Chang WT, Chang FR, Hung MY, Chiang TA, and Hung CY.** CD36 is a novel and potential anti-

fibrogenic target in albumin-induced renal proximal tubule fibrosis. *J Cell Biochem* 101: 735-744, 2007.

51. **Zager RA, Johnson AC, Hanson SY, and Shah VO.** Acute tubular injury causes dysregulation of cellular cholesterol transport proteins. *Am J Pathol* 163: 313-320, 2003.

52. **Zoja C, Donadelli R, Colleoni S, Figliuzzi M, Bonazzola S, Morigi M, and Remuzzi G.** Protein overload stimulates RANTES production by proximal tubular cells depending on NF-kappa B activation. *Kidney Int* 53: 1608-1615, 1998.

### FIGURE LEGENDS

Fig. 1. Dose-dependent endocytic association (A and B) and degradation (C and D) by HK-2 cells of  $^{125}\text{I}$ -HSA (A and C) and  $^{125}\text{I}$ -AOPPs-HSA (B and D). HK-2 cells were incubated at  $37^\circ\text{C}$  for 24 hr with the indicated concentrations of  $^{125}\text{I}$ -HSA and  $^{125}\text{I}$ -AOPPs-HSA in the presence (nonspecific:  $\square$ ) or absence (total:  $\circ$ ) of 50-fold excess amounts of the unlabeled ligands. The specific cell-association or degradation ( $\bullet$ ) was plotted after subtracting the non-specific values from the total values. Data represent the means  $\pm$  SD (n=6). \*  $P < 0.05$ , \*\*  $P < 0.01$  versus each specific cell-association or degradation of HSA.

Fig. 2. Effects of HSA on the endocytic association of  $^{125}\text{I}$ -AOPPs-HSA with HK-2 cells and of megalin siRNA transfection on the expression of megalin transcript and on the endocytic association of  $^{125}\text{I}$ -AOPPs-HSA with HK-2 cells. A: cells were incubated at  $37^\circ\text{C}$  for 24 hr with 0.5 mL of K-SFM medium containing  $2.5\ \mu\text{g/mL}$  of  $^{125}\text{I}$ -AOPPs-HSA in the absence or presence of  $125\ \mu\text{g/mL}$  of unlabeled AOPPs-HSA or HSA, followed by determination of endocytic association. Data represent the means  $\pm$  SD (n=5). \*  $P < 0.01$  versus control. B: immunoblot analyses of megalin in HK-2 cells transfected with 80 pmol megalin siRNA was performed using goat anti-human megalin

antibody (C19). The graphic representation of an immunoblot analysis demonstrated the effect of megalin siRNA on their protein expression in HK-2 cells. C: cells transfected with 80 pmol megalin siRNA were incubated at 37°C for 24 hr with 0.5 mL of K-SFM medium containing 2.5 µg/mL of <sup>125</sup>I-AOPPs-HSA, followed by the determination of any endocytic association. Data represent the means ± SD (n=4).

Fig. 3. Immunoblot analyses of A: CD36, B: SR-A, C: LOX-1, D: SR-B1, E: RAGE and F: Galectin-3 in HK-2 cells. Cellular proteins (10 µg) were subjected to an immunoblot analysis using anti-CD36 polyclonal antibody (1:100), anti-SR-A polyclonal antibody (1:200), LOX-1 antibody (1:1000), anti-SR-B1 polyclonal antibody (1:1000), anti-human RAGE polyclonal antibody (1:1400), anti-human galectin-3 polyclonal antibody (1:1000), or anti-β-actin polyclonal antibody (1:500). PC: Positive control (human macrophage: CD36, SR-A, LOX-1 and galectin-3; RAGE-CHO cells: RAGE; SR-B1-CHO-cells: SR-B1). All experiments were repeated three times with almost identical results.

Fig. 4. Dose-dependent endocytic association (A and B) and degradation (C and D) of <sup>125</sup>I-AOPPs-HSA by CD36-CHO cells (A and C) or mock-CHO cells (B and D). Cells were incubated for 37°C for 5 hr in 0.5 mL DMEM medium containing 3% BSA with concentrations of <sup>125</sup>I-AOPPs-HSA in the presence (nonspecific: □) or absence (total: ○) of 50-fold excess amounts of unlabeled ligands. The specific cell-association and degradation (●) were plotted after subtracting the non-specific values from the total values. Data represent the means ± SD (n=3). \* *P* < 0.01 versus each specific cell-

association or degradation of AOPPs-HSA in mock-CHO cells.

Fig. 5. Effect of anti-CD36 antibody (FA6-152) on the endocytic uptake of  $^{125}\text{I}$ -AOPPs-HSA by HK-2 cells. Cells were incubated at  $37^\circ\text{C}$  for 24 hr with 0.5 mL of K-SFM medium containing  $2.5\ \mu\text{g/mL}$  of  $^{125}\text{I}$ -AOPPs-HSA in the presence or absence of unlabeled AOPPs-HSA ( $125\ \mu\text{g/mL}$ ), anti-CD36 antibody (FA6-152:  $80\ \mu\text{g/mL}$ ), or control antibody (MOPC21:  $80\ \mu\text{g/mL}$ ) or HSA( $125\ \mu\text{g/mL}$ ). Results are the means  $\pm$  SD (n=3). \*  $P < 0.05$ , \*\*  $P < 0.01$  versus control.

Fig. 6. Expression of CD36 induced by AOPPs-HSA in HK-2 cells. Cell proteins ( $10\ \mu\text{g}$ ) were subjected to immunoblot analysis using anti-CD36 polyclonal antibody (L-17) (1:100), or anti- $\beta$ -actin polyclonal antibody (1:500). Results are the means  $\pm$  SD (n=3). \*  $P < 0.05$ , \*\*  $P < 0.01$  versus control cells.

Fig. 7. Assessment of reactive oxygen species (ROS) by fluorescence-activated cell sorter analysis. After CM- $\text{H}_2\text{DCFDA}$  incubation, HK-2 cells were treated with HSA or AOPPs-HSA for 15 min. Accumulation of DCF was measured with a flow cytometer by monitoring fluorescence at 526 nm. Intracellular ROS formation is expressed as a ratio of the mean fluorescence intensity of control cells incubated in an albumin-free medium. Results are the means  $\pm$  SD (n=5). [NAC]=20 mM. [DPI]=10  $\mu\text{M}$ . [Staurosporine] =100 nM. \*  $P < 0.05$ , \*\*  $P < 0.01$  versus control cells. #  $P < 0.01$  versus cells treated with 5 mg/mL HSA.

Fig. 8. Effect of anti-CD36 antibody (FA6-152) or ROS inhibitors on the TGF- $\beta$ 1 secretion induced by AOPPs-HSA. Cells were treated with HSA, AOPPs-HSA, or AOPPs-HSA in the presence of anti-CD36 antibody (FA6-152), NAC or DPI at 37°C for 24 hr. Results are the means  $\pm$  SD (n=3). \*  $P < 0.01$  versus control cells.

Fig. 1

Iwao Y et al.

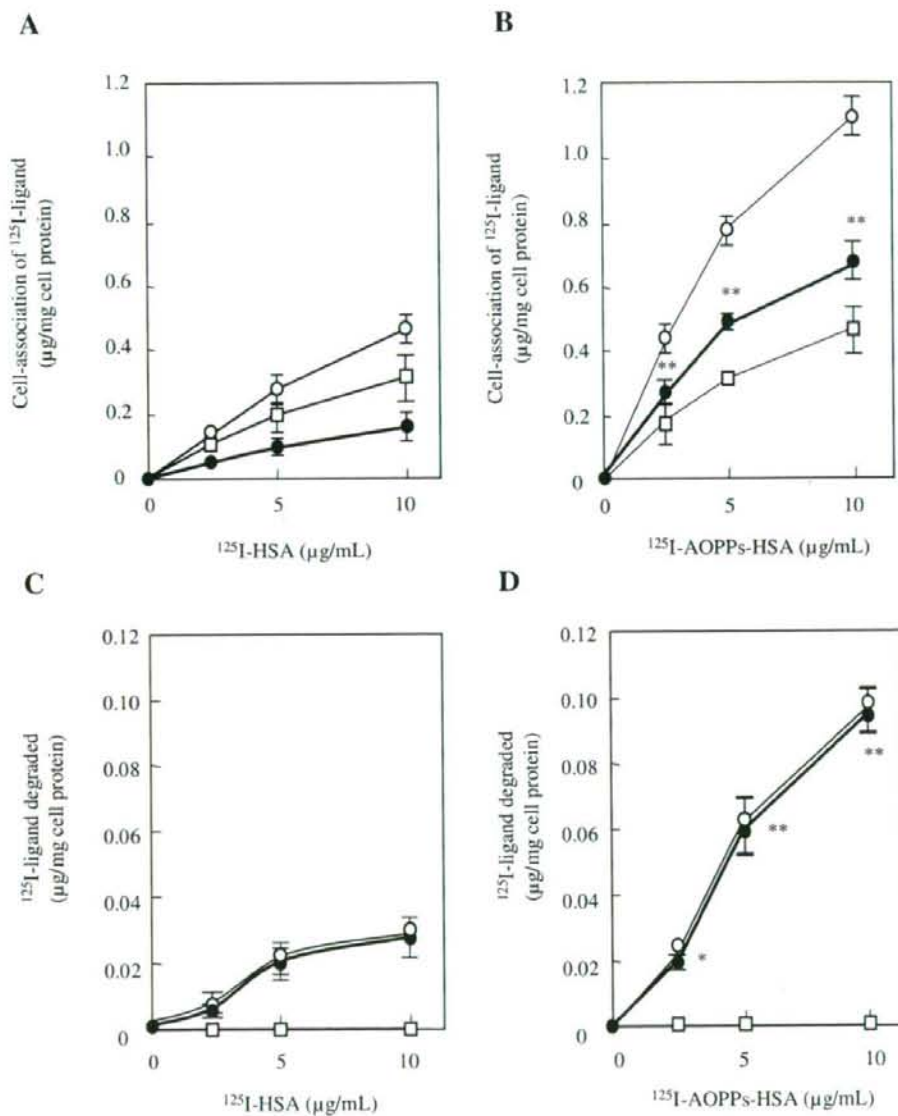
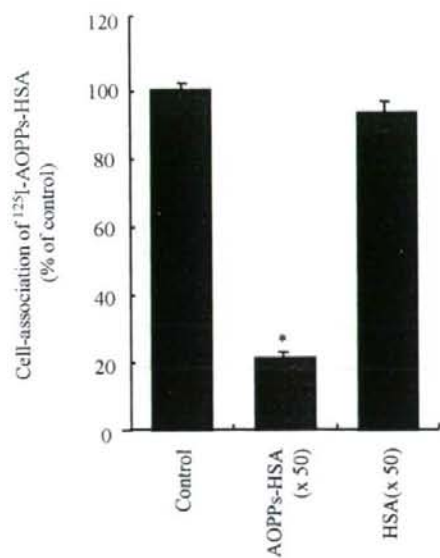


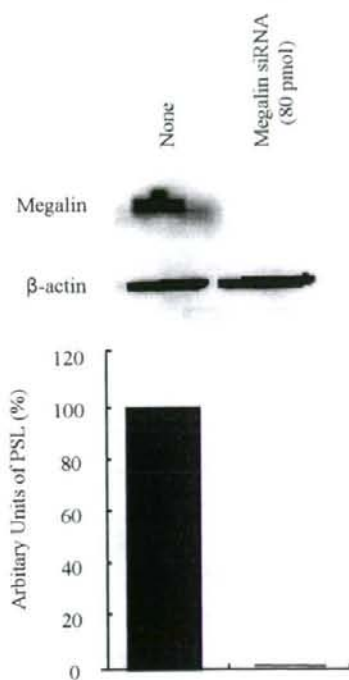
Fig. 2

Iwao Y et al.

A



B



C

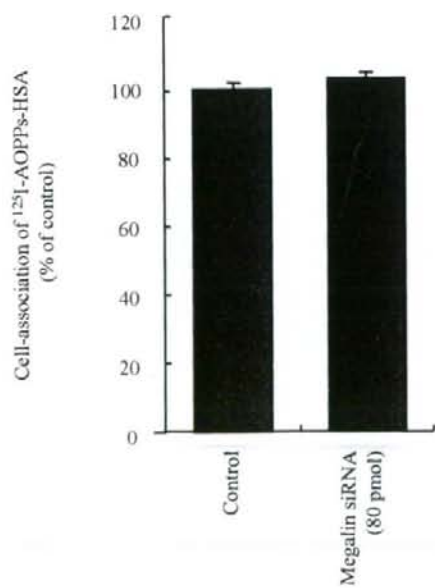




Fig. 3

Iwao Y et al.

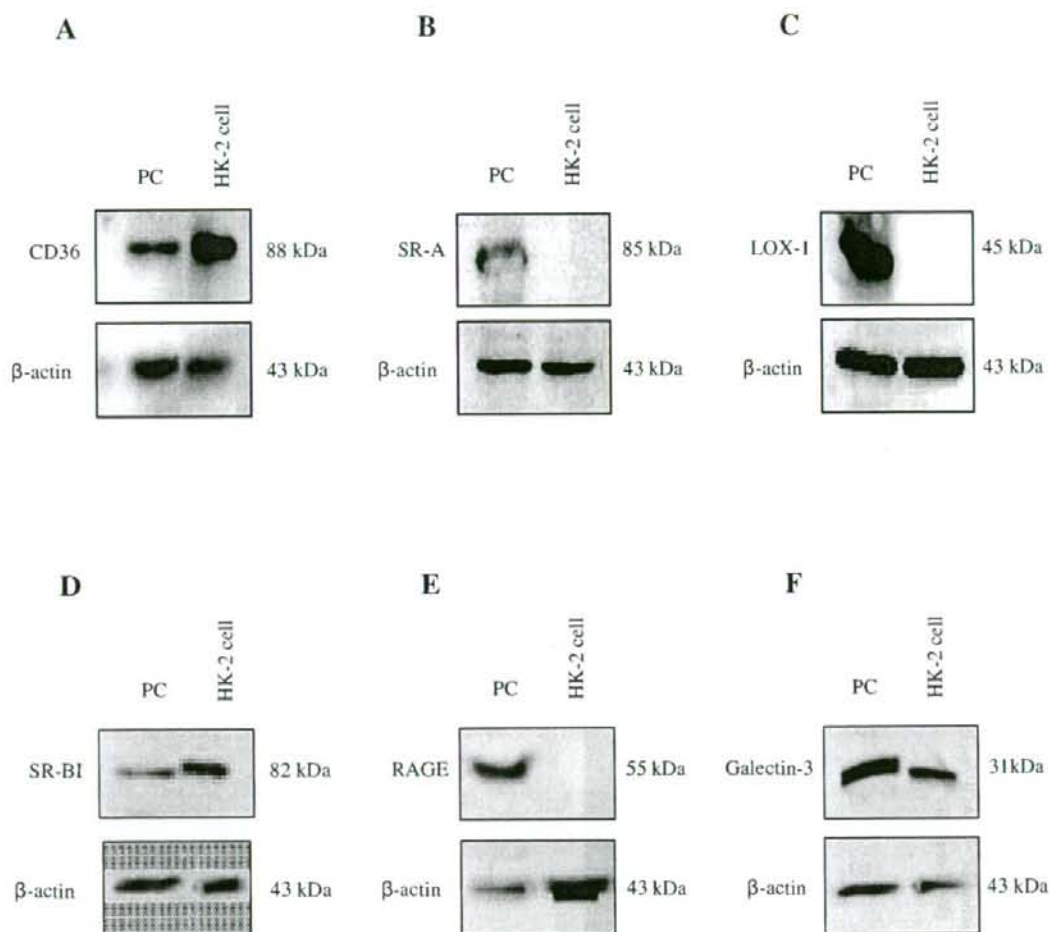


Fig. 4

Iwao Y et al.

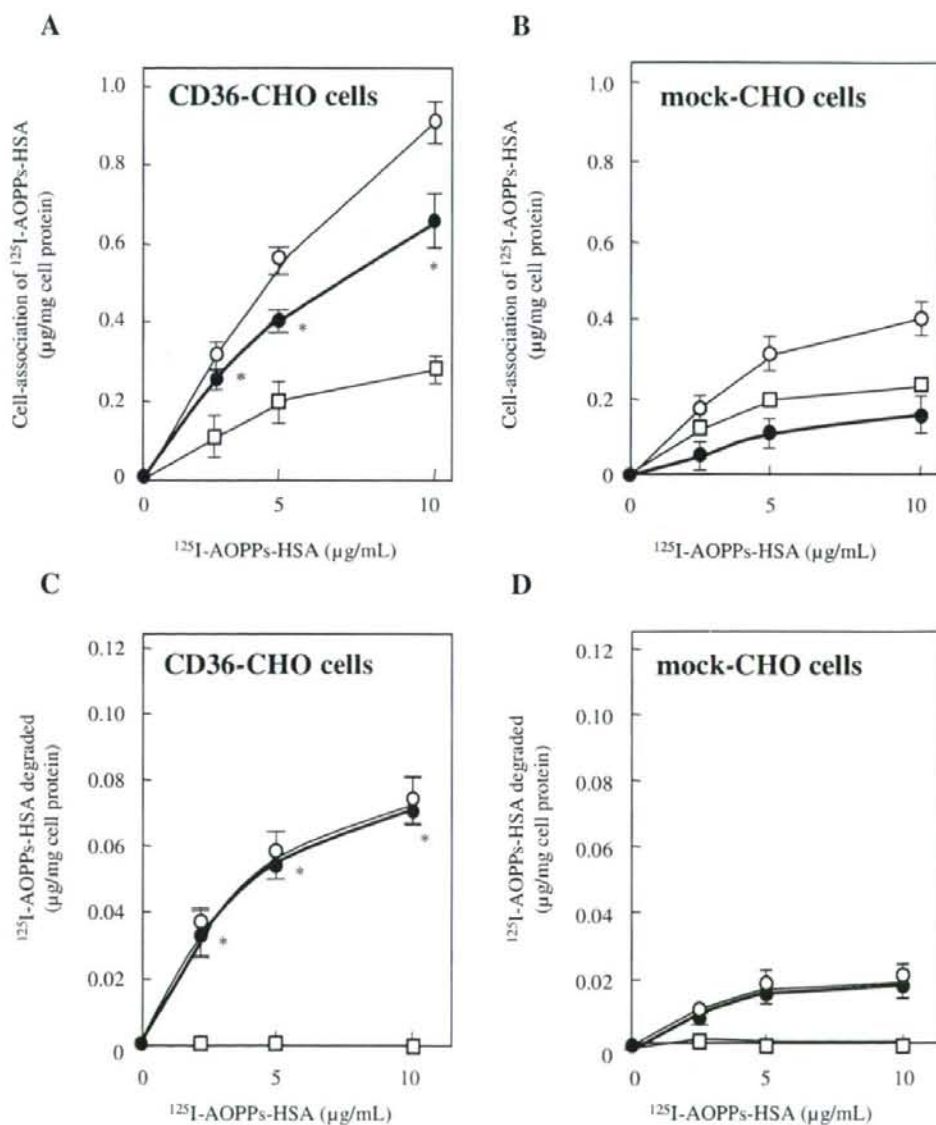


Fig. 5

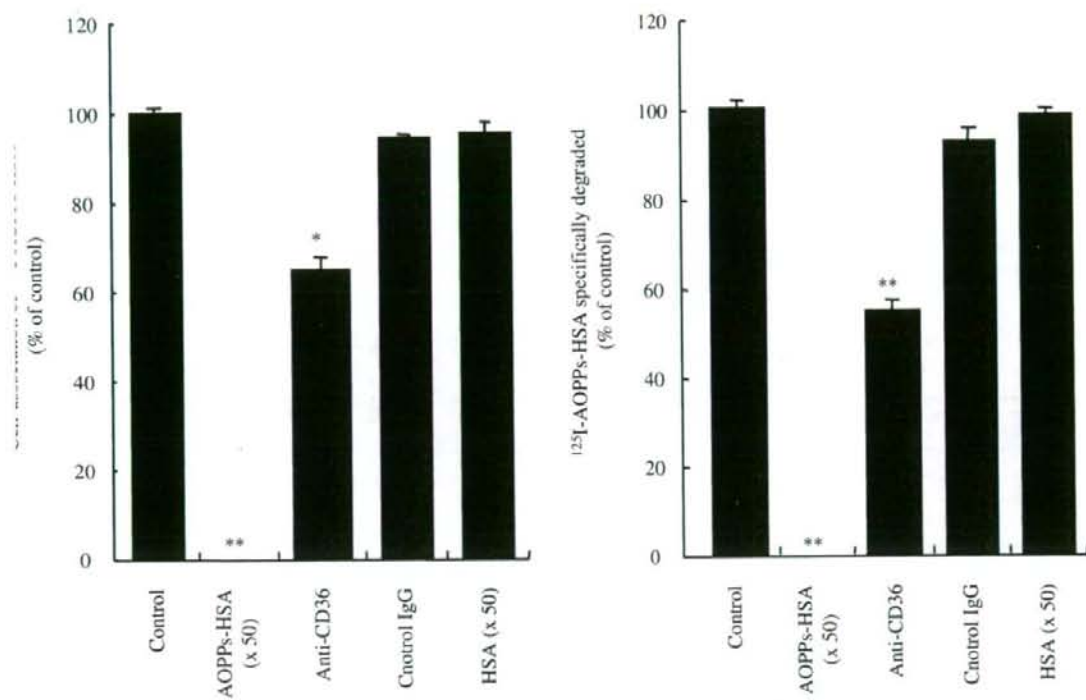
*Iwao Y et al.*

Fig. 6

Iwao Y et al.

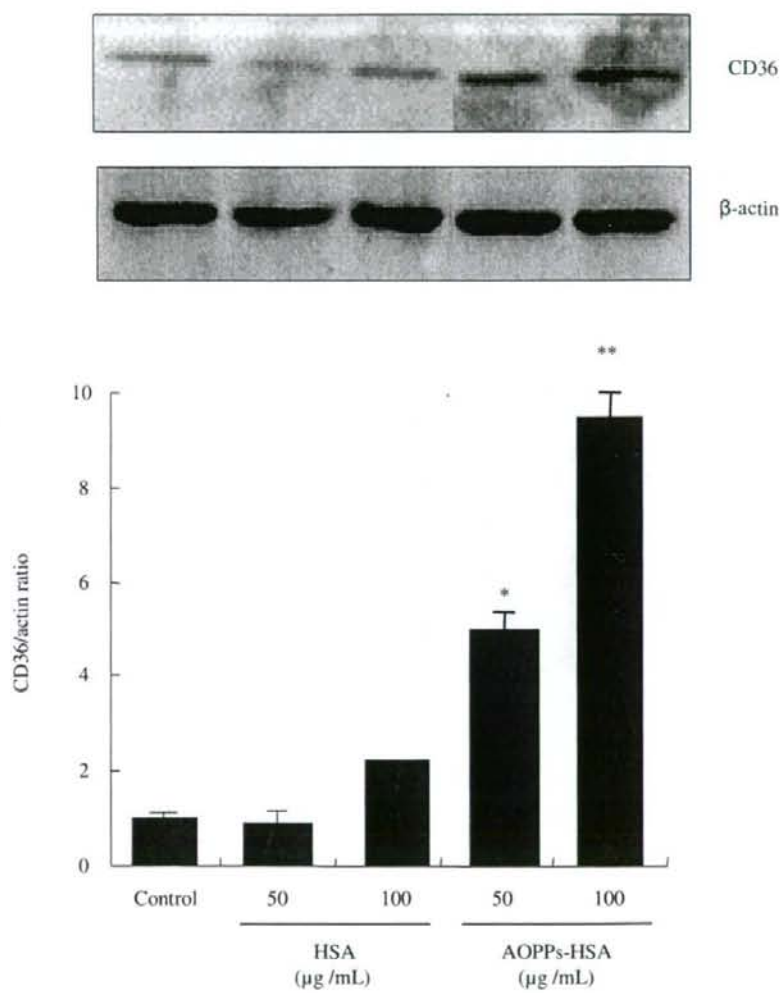


Fig. 7

Iwao Y et al.

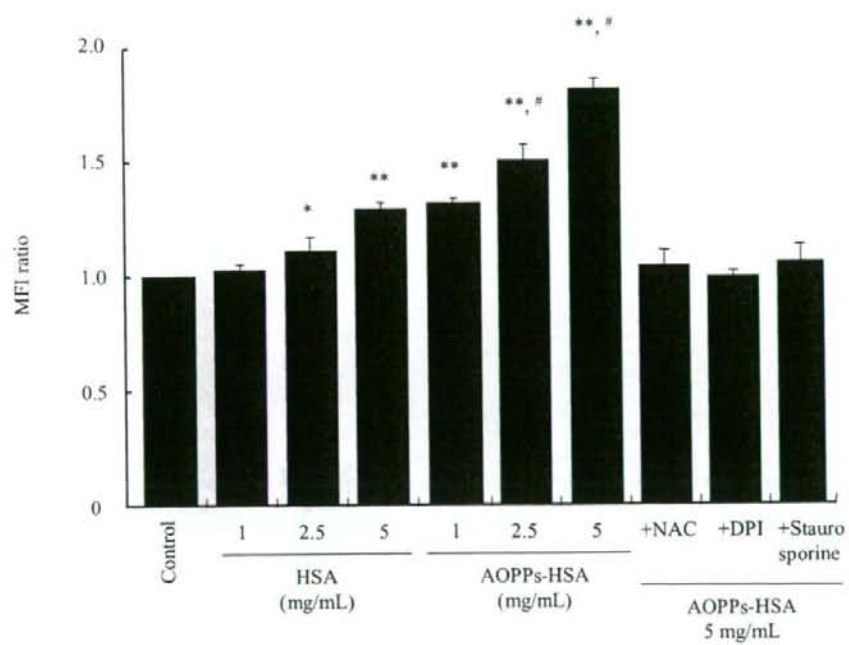


Fig. 8

Iwao Y et al.

